Lateral Migration of a Rigid Sphere in Torsional Flow of a Viscoelastic Fluid

A single polystyrene sphere of radius a, between 141 and 275 micron, when injected into a disk-plate (torsional) flow of polybutene (viscosity 36 poise, M_n ~680), migrates radially inward at a rate that is dramatically increased by dissolving 1% of a high-molecular-weight polyisobutylene (M_v ~10^6) to make the fluid viscoelastic. The torsional flow field was created by rotating a 21-cm-diameter disk at a rate ω of 6–9 rpm with a gap H of 3.7–5.4 mm between this and a ground glass plate with the fluid in the gap. Lateral migration toward a lower shear rate increased with increasing shear rate and with increasing shear rate gradient in the manner predicted by Brunn (1976) or Chan and Leal (1977). Shear rates up to 25 s^{-1} were investigated. Below a shear rate of 8 s^{-1} the radial migration velocity is of the form $v_r = -L(\omega a/H)^2 r$, where L is a positive constant containing the fluid properties, and r is the radial position of the particle.

T. E. KARIS, D. C. PRIEVE and S. L. ROSEN

Department of Chemical Engineering
Carnegie-Mellon University
Pittsburgh, PA 15213

SCOPE

During nonhomogeneous shear flow of a viscoelastic fluid, a rigid particle entrained by the fluid will migrate across the streamlines, even in the absence of external forces such as gravity or an electric field. Such migration affects the efficiency of capture of particles by grains of fibers in deep-bed or fibrous mat filters. Migration of additives or gel particles during extrusion of polymer melts might also be responsible for a phenomenon called "plate-out," which eventually leads to plugging of the die.

In this paper, we report direct visual observation of migration of a single spherical particle across the streamlines of torsional flow of a 1% w/w solution of a high-molecular-weight polyisobutylene in a low-molecular-weight polybutene solvent. The radial migration of the sphere is measured at different positions in the flow field for two different rotation speeds ω, two different plate separations H, and three different particle radii a. In a later paper we will report on the effect of fluid properties.

CONCLUSIONS AND SIGNIFICANCE

Except near the outer boundary of the rotating disk, the migration was always observed to occur in the direction of decreasing shear rate. For local shear rates less than 8 s^{-1}, the radial speed v_r was observed to be within 20% of $-v_r = L(\omega a/H)^2 r$, where $L = 0.027$ s for this fluid. The form of this equation was deduced from the more general theory developed by Brunn (1976) and Chan and Leal (1977). Further, we observed no significant dependence of the migration speed on the vertical position of the particle between the horizontal plates.

INTRODUCTION

Migration of particles across streamlines in a viscoelastic fluid is an important mechanism for the filtration of polymeric fluids. Currently, conventional filters with some design modifications are employed to remove solid contaminants from such fields. However, the mechanism by which the particles move laterally toward the collector in highly viscous polymer fluids is unlike that in water filtration, since diffusion or inertial impaction of macroscopic particles is unimportant in such viscous fluids. An understaning of the mechanism behind the lateral migration would be helpful for the design of an improved filter for these fluids.

On the other hand, particle migration often causes problems during extrusion of filled thermoplastic melts. Particle migration toward the machine surfaces gives rise to "plate-out," a deposit of additives (such as lubricants, plasticizers, stabilizers, pigments and fillers) which were originally dispersed in the plastic (Mascia, 1974; Throne, 1979). Briefly, the particles migrate toward and deposit on the machine surfaces, effectively altering their dimensions (Spinner and Simpson, 1971). Lippoldt (1978a,b) has examined chemical means for preventing plate-out. With knowledge of the migration mechanism, it might be possible to design the processing equipment to obtain flow fields which minimize migration or reverse its direction.

Table 1 shows previous observations on the rate and direction of the lateral migration in viscoelastic fluids. During steady shear of a viscoelastic fluid, normal stresses arise in addition to those generated by shear of a purely viscous fluid. Previous investigators have attributed the lateral migration to this additional stress. They found that the migration is toward a lower bulk shear rate and that increasing the particle size or the gradient of the bulk shear rate increrases the migration velocity. These trends are in quantitative agreement with predictions by Brunn (1976) and Chan and Leal (1977), which are based on the assumption of a second-order fluid.

This paper describes an investigation of a rigid sphere migrating radially in torsional flow of a polymer solution as a function of the particle radius, the rotation rate of the disk, the gap between the disk and the plate, and the radial position of the particle. The main contribution of this paper is to test the model of Brunn (1976), and Chan and Leal (1977) more quantitatively by systematically varying each experimental parameter and evaluating the order of dependence of the migration speed upon each parameter. For

Current Address: T. E. Karis, IBM Corp., K42/282, San Jose, CA 95193; S. L. Rosen, Dept. of Chem. Eng., Univ. of Toledo, Toledo, OH 43606.

TABLE 1. REVIEW OF PREVIOUS WORK

Flow Field Geometery	Direction of Migration	Rate of Migration	References
Tube	Toward the Center of the Tube	Increases with Increasing Radial Position and Particle Size	Karnis et al., 1963 Karnis, 1966 Karnis & Mason, 1966 Gauthier et al., 1971b
Couette	Toward the Outer Cylinder	Increases with Increasing Velocity Gradient. Decreases with Increasing Radial Position	Karnis, 1966 Highgate & Whorlow, 1969 Gauthier et al., 1971a Bartram, 1973 Bartram et al., 1975
Cone-Plate	Radially Outward		Highgate, 1966 Highgate & Whorlow, 1968 Highgate & Whorlow, 1969
Extrusion Through a Die	Laterally into the Recirculation Zones		Walker, 1965 Giesekus, 1969 Karmer & Reher, 1978

shear rates less than about 8 s^{-1}, experiment and theory agree within the experimental error over the range of parameters studied.

THEORY

Lateral Migration

Theoretical predictions of the migration velocity have been developed for fluids whose response to stress follows the second-order constitutive equation (Coleman and Markovitz, 1964; Bird et al., 1977):

$$T = -\eta\gamma + a_2\left[\frac{D\gamma}{Dt} + \tfrac{1}{2}(\Omega\cdot\gamma - \gamma\cdot\Omega)\right] - a_{11}\gamma\cdot\gamma, \quad (1)$$

where T is the deviatoric stress, $\gamma \equiv \nabla v' + (\nabla v')^T$ is the rate of strain or the symmetric part of $\nabla v'$, v' is the fluid velocity, $\Omega \equiv \nabla v' - (\nabla v')^T$ is the antisymmetric part of $\nabla v'$, D/Dt denotes the material derivative, and η, a_2 and a_{11} are the scalar parameters characteristic of the fluid. Most fluids behave according to Eq. 1 if the shear rate is small enough. In addition, the migration predictions assume a small particle-Reynolds-number and a small Weissenberg number (ratio of normal to shear stresses).

Brunn (1976) and Chan and Leal (1977) independently solved for the disturbance to the velocity and stress fields caused by the particle's presence. They obtained a solution to the equations of motion as a regular perturbation expansion, treating the ratio of the fluid's relaxation time to the processing time as a small parameter. As boundary conditions, they assume the disturbance vanishes far from the particle and no slip at the particle's surface. Given the undisturbed flow field v', the migration velocity v (relative to v') of a rigid sphere of radius entrained in this flow, was found to be

$$v = k_1\nabla^2 v' + k_2\gamma\cdot\nabla^2 v' + k_3 E{:}\gamma + k_4\epsilon{:}(\gamma\cdot\Omega), \quad (2)$$

where E is the symmetric irreducible part of $\nabla\nabla v'$, ϵ is the alternating unit tensor, and the scalars k_i (which are all proportional to a^2) depend only on the rheological parameters and on the particle radius. By comparing the results of Brunn (1976) and Chan and Leal (1977), Brunn (1980) concluded that they differ only in the expression for k_2, and then only by at most 10%.

For the simple torsional flow shown in Figure 1, the undisturbed velocity field is

$$v' = \frac{\omega r z}{H} e_\theta \quad (3)$$

where e_θ is the unit vector in cylindrical coordinates (r,θ,z).

We converted Eq. 3 into cartesian coordinates, and substituted it into Eq. 2. The cartesian components of the tensors, as well as the results of the indicated operations, were deduced with the aid of MACSYMA (Project MAC's SYmbolic MAnipulation system, Laboratory for Computer Science, MIT), an advanced computer language for symbolic manipulation.

The migration velocity thus obtained is:

$$v = -Are_r, \quad (4)$$

where

$$A = L\left(\frac{\omega a}{H}\right)^2 \quad (5)$$

and

$$L = \frac{5}{126}\frac{10a_2 - a_{11}}{\eta}. \quad (6)$$

For any given fluid, L is constant and v_r is proportional to $(\omega a/H)^2 r$. In this paper, we systematically vary each of these parameters to test this relationship for one fluid.

Secondary Flow

In rotational devices, such as the disk and plate, there is the possibility that the particle motion is due to convection in the radial direction. When $\nabla\times\nabla\gamma = 0$ (which holds for the velocity field of Eq. 3), Savins and Metzner (1970) conclude that the secondary flow of a second-order fluid will be the same as that of a Newtonian fluid. These same authors deduced the secondary flow of a Newtonian fluid, caused by the rotation of an infinite disk, by means of a perturbation expansion in N_{Re}. They obtained the leading term

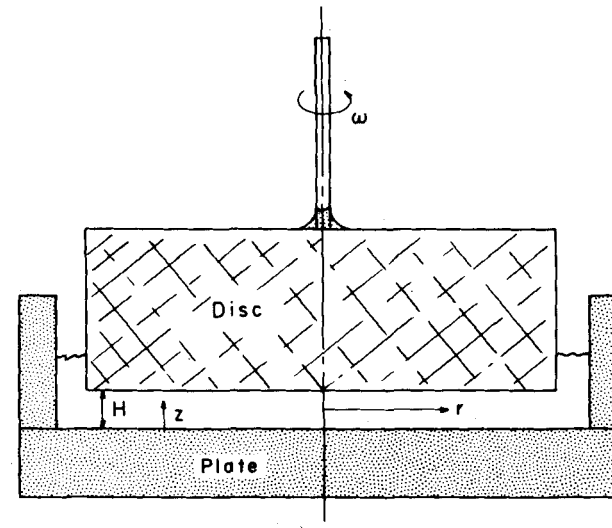

Figure 1. Side view in the cross section of the torsional flow apparatus. A disk with a 21 cm diameter is rotated at 6–9 rpm parallel to a stationary plate. The separation H is 3.7–5.4 mm. A single rigid sphere is injected into the fluid held between the disk and the plate.

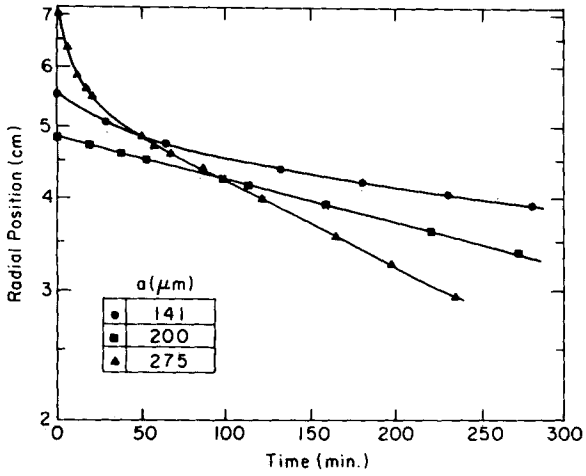

Figure 2. Typical trajectories $r(t)$ for three different particles. Points denote raw data while solid curves denote an empirical fit of Eq. 8 to data. Note that the particles migrate radially across streamlines toward the axis of rotation of the disk. The fluid is 1% PIB in PB at 30.5°C, ω = 8.82 rpm, H = 5.4 mm.

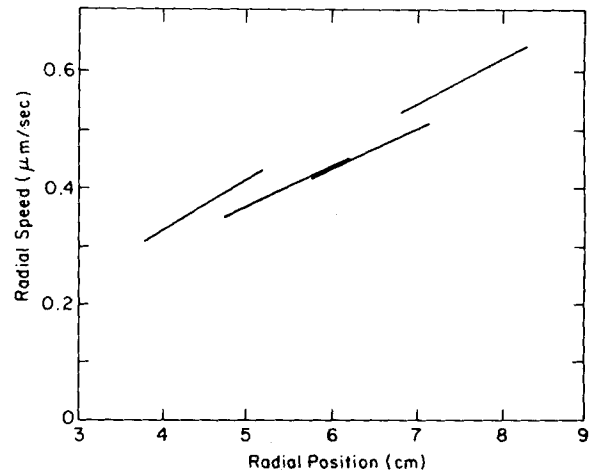

Figure 4. Rate of migration of a 315 μm sphere through the solvent PB at 30.5°C, ω = 8.82 rpm, H = 3.7 mm. Although migration still occurs, the rate is much less than when PIB is dissolved (Figure 3).

of the expansion and experimentally demonstrated reasonable agreement between the inward velocity of the fluid deduced from their approximate solution. Later, McCoy and Denn (1971) obtained both a numerical solution and a two-term approximation for the secondary flow in the disk-plate geometry. They demonstrated reasonable agreement between the numerical solution and the two-term approximation when $R/H > 10$ and $N_{Re} < 0.5$. These analyses predict outflow near the rotating disk and inflow near the stationary plate. Only the rate at which the fluid is flowing radially inward is needed here to establish a criterion for neglecting secondary flow. The two-term approximation of McCoy and Denn (1971) gives the maximum speed at $z/H = 0.192$; this maximum speed is

$$v_r = -0.00854 \frac{\rho\omega^2 H^2}{\eta} r. \tag{7}$$

Migration velocities in the viscoelastic fluids were much higher than the maximum fluid velocity calculated from Eq. 7.

A more detailed analysis of secondary flow in the disk-plate geometry, which predicts secondary flow cells of toroidal shape at higher Reynolds numbers, was done by Roberts and Shipman (1976). However, for the experiments discussed here $N_{Re} < 0.005$, which is much smaller than that used in their calculations. The most compelling reason for ruling out any significant effect of secondary flow in the following experiments is that inward migration was observed at all evaluations whereas the simple consideration of conservation of fluid requires any secondary flow to be radially inward at some elevations and radially outward at others.

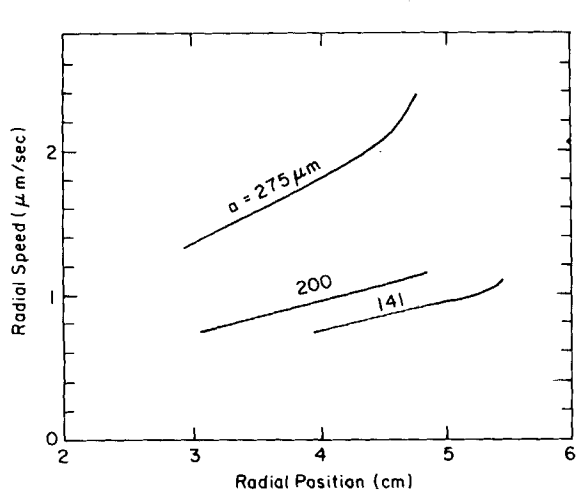

Figure 3. Rate of inward radial migration obtained by differentiating the solid curves in Figure 2. At the same radial position, larger particles migrate faster.

EXPERIMENT

Apparatus

The disk-plate geometry was chosen because it provides a constant shear-rate gradient that is orthogonal to concentric circular streamlines, and a long radial span over which to observe the particle trajectory so that the observer does not have to move with the particle. In addition, there is no refraction: the position of the particle is observed through a flat surface.

A clear plastic disk, 3 cm thick and 21 cm in diameter, was fabricated and attached to a constant-speed motor with a steel shaft. The body of the disk was made from polyester casting resin in a circular mold with a Plexiglas base and a Teflon wall. Prior to casting, concentric circular rings 1 cm apart were engraved in the Plexiglas disk, which were later used to determine the radial position of the particle. After the resin had set, the disk adhered firmly to the Plexiglas, and the Teflon wall was peeled away. Once the rough-cast disk was cured and annealed, a collar was bolted to the cast part and the $\frac{3}{8}$ in. (9.5 mm) diameter steel shaft was fixed to the collar. To ensure that the disk and shaft assembly rotates over the plate without squeezing the fluid in and out, the shaft and the lower surface of the disk must be perpendicular to one another. This was achieved by machining the surfaces flat (to within 5 mil) with the shaft in a lathe chuck, and then polishing with carbide paper and alumina grit.

Since the particle was more visible from above when illuminated from below, the plate was made from a piece of ground glass. To contain the fluid, a circular Plexiglas dike (1.8 cm high and 2 cm from the outer edge of the disk) was glued to the upper surface of the glass plate. Water from a constant-temperature water bath was circulated through a Plexiglas chamber beneath the plate to maintain the temperature in the gap.

Materials

The experimental fluid must be transparent so that the particle can be observed. In addition, a set of experiments in a given fluid may last several weeks so the solvent must be nonvolatile. To minimize the secondary flow and sedimentation of the particle, a highly viscous solvent is desirable. Cross linking and shear degradation often lead to changes in the molecular weight distribution of dissolved high-molecular-weight polymer, which alters the elastic properties of the solution. The fluid must not greatly swell the solid sphere or dissolve the disk. Finally, the rheological behavior of the fluid should be adequately described by the second-order fluid model.

Certain polymer solutions at room temperature are rheologically similar to polymer melts at high temperature and are nearly ideal second-order fluids (Boger and Nguyen, 1978). Several polymer solutions were tested. Silicone oils, aqueous polyacrylamide solutions, and solutions of polyacrylamide in glucose were found to be unsatisfactory. Silicone oil is undesirable because it is difficult to clean off the apparatus, and evaporation

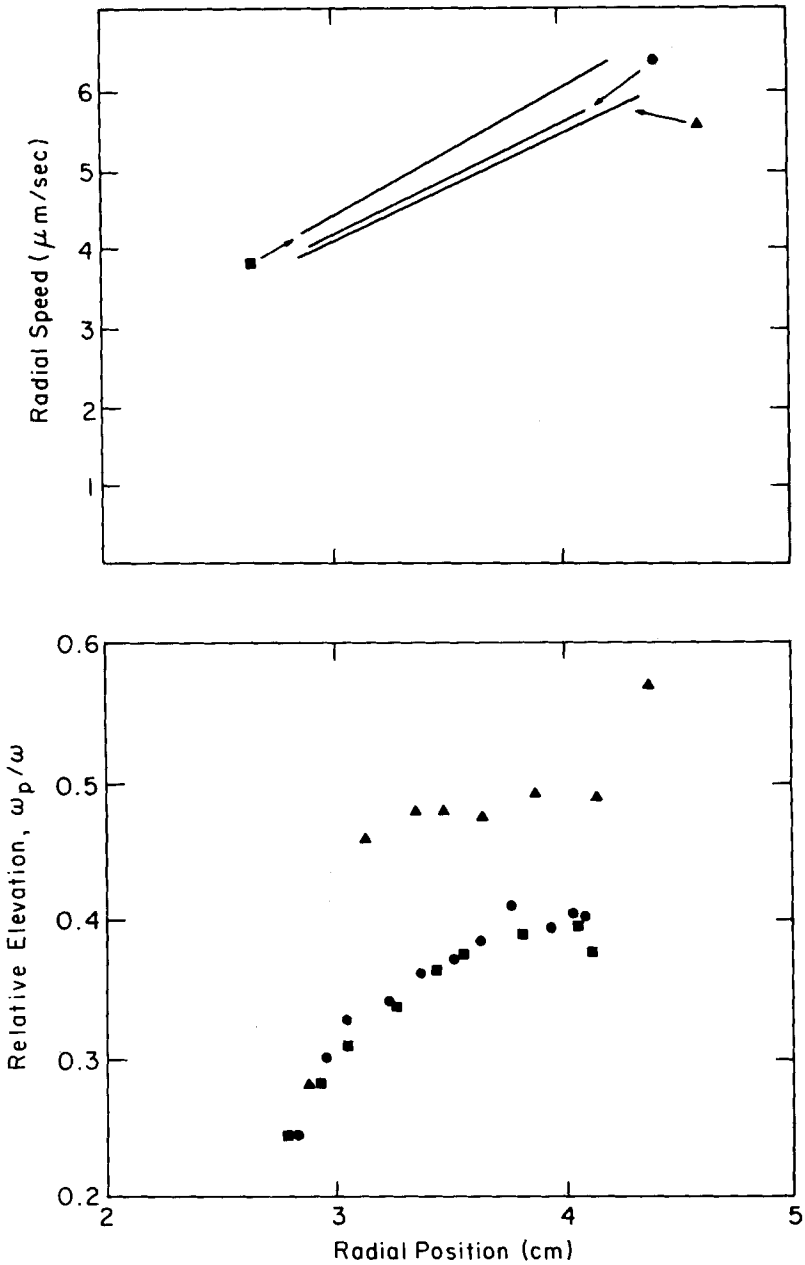

Figure 5. The effect of particle elevation on the migration rate of a 275 μm particle in a solution of 1% PIB at 30.5°C, ω = 8.82 rpm, H = 3.7 mm. Although the run denoted by triangles has a higher elevation than the other two runs, the velocity at any radial position is within experimental error of the other two runs.

concentrates solutions which contain water. Eventually, a solution of high-molecular-weight polyisobutylene (PIB, Enjay Vistanex L-120) in polybutene (PB, Amoco) was selected as the best fluid. Since the PIB dissolved very slowly in such a viscous solvent, the PIB was first dissolved in reagent grade heptane. This solution was added to the PB and then the heptane was removed in a vacuum oven, leaving the PIB dissolved in the PB. The solvent PB had the following properties:

- A viscosity of 36 poise (3.6 Pa-s) at 30.5°C (determined with a Cannon-Fenske Routine capillary viscometer).
- A number-average molecular weight of 680 (estimated from the viscosity by means of data supplied by the manufacturer: "Storage and Handling: Amoco Polybutenes," Bulletin 12G, 1981).
- A density of 0.884 g/cm^3 (measured with a pycnometer).

Similar polybutenes have been used by the National Bureau of Standards as Newtonian calibrating liquids for viscometers (Hardy, 1962). The experimental fluid was 1% w/w PIB (viscosity-average molecular weight 10^6) in PB.

Addition of PIB to the PB significantly changed the properties of the fluid. The viscosity increased to 90 poise (9 Pa-s) and the solution tended to climb several millimeters up a rotating vertical rod, whereas the solvent alone displayed no rod-climbing tendency. Steady-shear tests in a cone-plate viscometer indicated that the viscosity of the solution remained independent of shear rate for shear rates less than 100 s^{-1}. The rod-climbing height was measured at 30°C for different rotation speeds using a 9-mm-diameter rod. As expected for a second-order fluid, the height was proportional to the square of the rotation speed for speeds less than 100 rpm. The proportionality constant was 0.0021 cm-s^2. Using a surface tension of 32 dyne (0.32 mN)/cm and a density of 0.9 g/cm^3 in the analysis of Beavers and Joseph (1975), this rod-climbing behavior implies $2a_{11} - 3a_2 = 2.5$ g/cm.

This fluid was also subjected to small-amplitude oscillatory motion in a cone-plate device (Rheometrics model RMS-7200 Mechanical Spectrometer). The stress and the phase lag between deformation and stress were analyzed with the aid of an on-line data acquisition system to determine the dynamic shear-moduli, G' and G'', as a function of the frequency ω of oscillatory motion over the range 0.2–3 Hz. As expected for a second-order fluid, a plot of $\ln G''$ vs. $\ln \omega$ was linear with a slope of 0.98 ± 0.03. The intercept yields a value of the viscosity which is within experimental error of the value obtained with the capillary viscometer. However, instead of 2.0, a linear regression of $\ln G'$ vs. $\ln \omega$ yielded a slope of 1.56 ± 0.06. Thus the response of the fluid to dynamic shear is not entirely consistent with a second-order model.

The particles were polystyrene-divinylbenzene Microspheres (cat. no. 433, Duke Scientific Co.), with a density of 1.05 g/cm^3. For any experiment, a single particle was selected from the lot. The diameter of the sphere was

measured to within 5 μm by optical microscopy while immersed in the fluid. The hydrodynamic radius (determined by sedimentation in a 1.4 cm-diameter tube) was within 4% of the radius meaured by microscopy.

Procedure

First, the disk was aligned parallel to the plate to within 0.1 mm of the desired gap with feeler gauges (Figure 1). The temperature in the gap was measured before and after each run with a miniature thermocouple probe. When the room temperature was kept within 5°C of the bath, the temperature in the gap was uniform and reproducible to within ±0.5°C. To begin the experiment, a particle of known diameter was drawn into a 6-in.-long (152 mm), 18-gauge needle and injected at the desired radial and vertical position in the gap before beginning the rotation of the disk. The radial position of the particle was measured to within 0.1 cm by direct visual observation. The vertical position was deduced by comparing the period of revolution of the particle about the axis of the disk with the period of rotation of the disk.

Data Analysis

To determine v_r as a function of r, it was necessary to differentiate the radial trajectory with respect to time. Equation 4 predicts that $ln(r)$ should be a linear function of time t. However, as shown in Figure 2, there often was some deviation from linearity at larger r. Consequently, the data were fit to a linear equation with a correction term:

$$ln(r) = -At + B + C\exp(-t/\tau). \quad (8)$$

When the sum of the squares of the errors was less for a linear fit, C was set to zero. The constant A in Eq. 8 is also the A in Eq. 4.

RESULTS AND DISCUSSION

Three typical sets of data are shown in Figure 2 along with the corresponding empirical curves determined by a least-squares fit of Eq. 8. Besides the goodness of fit, one can notice that the curves become linear for $r \leq 5$ cm, which corresponds to $\gamma \leq 8\ s^{-1}$. For other rotation speeds or disk-plate separations this maximum r for linear dependence of $ln(r)$ on t was different, but the corresponding maximum shear rate γ remained about 8 s^{-1}.

Figure 3 shows the radial speed at different radial positions, obtained by differentiating the smooth curves in Figure 2. Owing to the form of Eq. 8 when $t \gg \tau$, the curves in Figure 3 must extrapolate to $dr/dt = 0$ at $r = 0$, which Figure 2 already demonstrated is consistent with the experimental data. At a given radial position, Figure 3 shows the migration rate is larger for larger particles. If the radial motion were due to radial convection, no dependence on particle size would be expected.

To demonstrate that migration of the rigid particle is caused by the polymeric solute, a few migration experiments were performed using pure solvent. The results are shown in Figure 4. The four curves correspond to four different starting locations. Although inward migration does occur in pure solvent, the speed is substantially slower than with dissolved polymer, despite the larger shear rates, the larger particle, and the smaller viscosity. At $r = 4$ cm, the 275 μm particle in Figure 3 migrates at a speed which is seven times that of the 315 μm particle of Figure 4.

Figure 5 shows that the elevation had an insignificant effect on the migration velocity. The elevation of the particle above the bottom plate was determined by comparing the angular velocity of the particle ω_p with that of the rotating disk ω. The ratio ω_p/ω should vary monotonically between zero, when the particle touches the stationary plate, and unity, when the particle touches the rotating disk. In Figure 5b, different symbols are used to denote different runs for the same particle under the same conditions. Sedimentation of the particle causes ω_p/ω to decrease with time. Note that the runs denoted by triangles occurred at a higher evaluation than the runs denoted by circles or squares. Despite the different elevations, Fig. 5a shows that the corresponding migration speeds are practically identical. Differences in migration speed between the two runs probably reflects the uncertainty in determining the speed by this method. Additional runs were performed

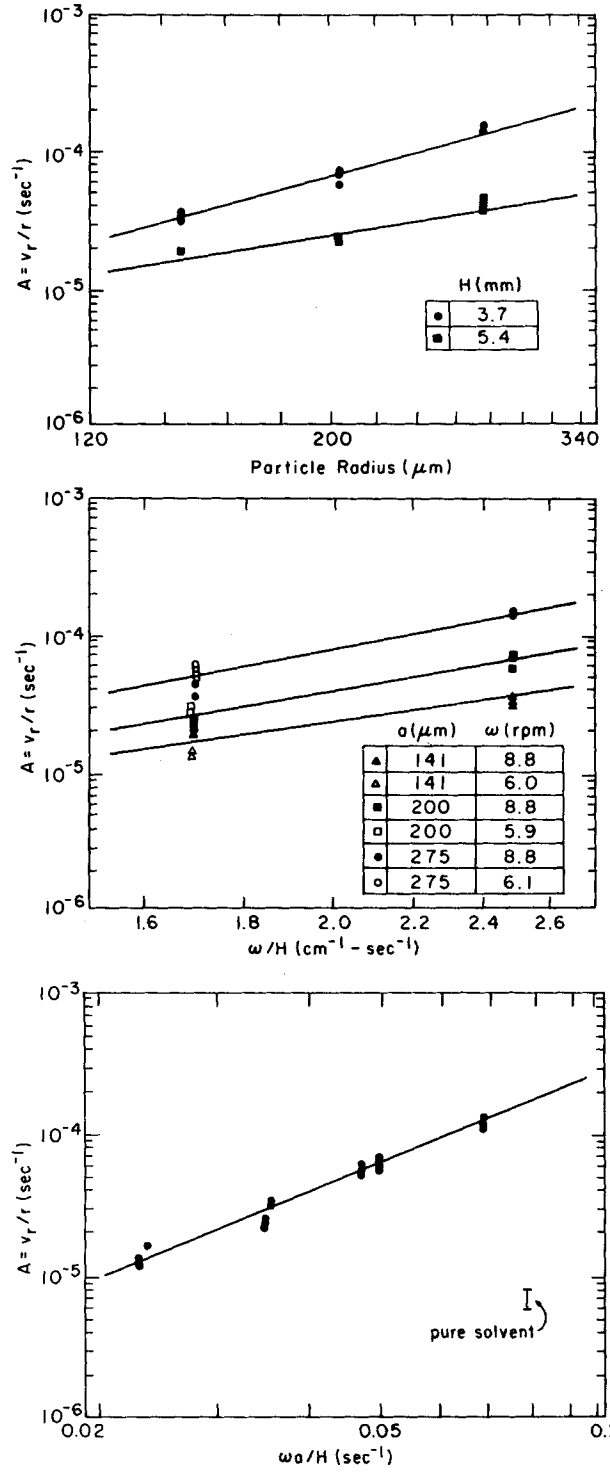

Figure 6. A comparison of the observed migration velocities with those predicted using Eqs. 4 and 5. If the predictions are correct, the slope of these six lines should be 2. The slope and confidence interval obtained for each line is listed in Table 2.

for higher elevations: in no case was outward migration observed, although any radial convection is expected to be directed outward near the rotating disk. Lack of dependence on elevation is further evidence that convection is not responsible for the radial migration of the particle. Moreover, the migration speed decreased with an increase in H; whereas convection is expected to increase (Eq. 7).

Since migration appears to be attributable to the elasticity of the polymer solution, we tested the ability of Eqs. 4 and 5 to predict the migration speed. Figures 3, 4, and 5 have already demonstrated that the radial velocity is directed inward and is proportional to

TABLE 2. SLOPES OF THE LINES IN FIGURE 6

Curve	Slope	Half Width of 90% Confidence Interval
Figure 6a		
H = 3.7 mm	2.15	0.20
H = 5.4 mm	1.2	0.6
Figure 6b		
a = 275 μm	2.7	0.5
a = 200 μm	2.5	0.5
a = 141 μm	2.0	0.6
Figure 6c	2.12	0.21

r (if the shear rate is not too large), which agrees with Eq. 4. Figure 6 shows the dependence on the particle radius a, the rotation rate of the disk ω, and the distance separating the disk and plate H. The ordinate for these graphs is the parameter A, obtained by a least-squares fit of the trajectory Eq. 8, which is also the coefficient A appearing in Eqs. 4 and 5. The straight lines were determined by a linear least-squares fit of the appropriate set of points. The slope of each line is reported in Table 2 along with its 90% confidence interval. According to Eq. 5, all of these slopes should be 2.00. The 90% confidence interval for four out of the six lines does include 2.00. In particular, the line of Figure 6c—which correlates all 31 sets of data—has a slope of nearly 2.00. Thus, Eqs. 4 and 5 with L = 0.027 s (the antilog of the y-intercept of the line in Figure 6c) adequately predicts all of the results observed for $\gamma \leq 8\ s^{-1}$.

ACKNOWLEDGMENT

T.E.K. was supported by a fellowship from The Brunswick Foundation.

NOTATION

A = particle velocity coefficient, Eq. 5
a = radius of a spherical particle
B,C = constants in Eq. 8
H = distance separating the disk from the plate
L = lumped elastic parameter, Eq. 6
M_n = number average molecular weight
M_v = viscosity average molecular weight
N_{Re} = Reynolds number, $\rho\omega H^2/\eta$
R = radius of the disk
r = radial position
t = time
v = particle velocity
v' = fluid velocity
z = elevation above the plate

Greek Letters

a_2,a_{11} = rheological constants for second-order fluid
η = viscosity of solution
ρ = density of the fluid
γ = local shear rate
τ = constant in Eq. 8
ω = rotation rate of the disk
ω_p = rate of revolution of the particle about the axis of disk rotation

LITERATURE CITED

Bartram, E., "Phenomenological Behavior of Particles in Newtonian and Non-Newtonian Liquids," Master's Thesis, McGill Univ. (1973).
Bartram, E., H. L. Goldsmith, and S. G. Mason, "Particle Motions in Non-Newtonian Media. III: Further Observations in Elastoviscous Fluids," *Rheol. Acta*, **14**, 776 (1975).
Beavers, G. S., and D. D. Joseph, "The Rotating Rod Viscometer," *J Fluid Mech.*, **69**, 475 (1975).
Bird, R. B., R. C. Armstrong, and O. Hassager, "*Dynamics of Polymeric Fluids*," *1 Fluid Mechanics*, Wiley (1977).
Boger, D. V., and H. Nguyen, "A Model Viscoelastic Fluid," *Polym. Eng. Sci.*, **18**, 1037 (1978).
Brunn, P., "The Behavior of a Sphere in Non-Homogeneous Flows of a Viscoelastic Fluid," *Rheol. Acta*, **15**, 589 (1976).
Brunn, P., "The Motion of Rigid Particles in Viscoelastic Fluids," *J. Non-Newt. Fluid Mech.*, **7**, 271 (1980).
Chan, P. C.-H., and L. G. Leal, "A Note on the Motion of a Spherical Particle in a General Quadratic Flow of a Second-Order Fluid," *J. Fluid Mech.*, **82**, 549 (1977).
Coleman, B. D., and H. Markovitz, "Normal Stress Effects in Second-Order Fluids," *J. Appl. Phys.*, **35**, 1 (1964).
Gauthier, F., H. L. Goldsmith, and S. G. Mason, "Particle Motions in Non-Newtonian Media. I. Couette Flow," *Rheol. Acta*, **10**, 344 (1971a).
Gauthier, F., H. L. Goldsmith, and S. G. Mason, "Particle Motions in Non-Newtonian Media. II. Poiseuille Flow," *Trans. Soc. Rheol.*, **15**, 297 (1971b).
Giesekus, V. H., "Verschiedene Phanomene in Stromungen Viskoelastischer Flussigkeiten Durch Dusen," *Rheol. Acta*, **8**, 411 (1969).
Hardy, R. C., "NBS Viscometer Calibrating Liquids and Capillary Tube Viscometers," National Bureau of Standards, *Monograph 55* (1962).
Highgate, D. J., "Particle Migration in Cone-Plate Viscometry of Suspensions," *Nature*, **211**, 1390 (1966).
Highgate, D. J., and R. W. Whorlow, "End Effects and Particle Migration in Concentric Cylinder Rheometry," *Rheol. Acta*, **8**, 142 (1969).
Karmer, R., and E-O. Reher, "Experimentelle Untersuchungen Zun Austrag von Gasblasen und Feststoffteilchen aus der Stromung Viskoelastischer vor Lochblenden," *Rheol. Acta*, **17**, 511 (1978).
Karnis, A., H. L. Goldsmith, and S. G. Mason, "Axial Migration of Particles in Poiseuille Flow," *Nature*, **200**, 159 (1963).
Karnis, A., "The Flow of Suspensions Through Tubes," PhD Thesis, McGill Univ. (1966).
Karnis, A., and S. G. Mason, "Particle Motions in Sheared Suspensions. XIX. Viscoelastic Media," *Trans. Soc. Rheol.*, **10**(2), 571 (1966).
Leal, L. G., "The Motion of Small Particles in Non-Newtonian Fluids," *J. Non-Newt. Fluid Mech.*, **5**, 33 (1979).
Lippoldt, R. F., "Postulated Mechanism for Plate-Out From PVC Processing Systems," *Soc. Plast. Eng. Tech. Pap.*, **24**, 737 (1978a).
Lippoldt, R. F., "How to Avoid Plate-Out in Extruders," *Plast. Eng.*, **34**(9), 37 (1978b).
Mascia, L., *The Role of Additives in Plastics*, Wiley (1974).
McCoy, D. H., and M. M. Denn, "Secondary Flow in a Parallel-Disk Viscometer," *Rheol. Acta*, **10**, 408 (1971).
Roberts, S. M., and J. S. Shipman, "Computation of the Flow Between a Rotating and a Stationary Disk," *J. Fluid Mech.*, **73**, 53 (1976).
Savins, J. G., and A. B. Metzner, "Radial (Secondary) Flows in Rheogoniometric Devices," *Rheol. Acta*, **9**, 365 (1970).
Spinner, S. H., and W. G. Simpson, *Plastics: Surface and Finish*, Butterworths, London (1971).
Throne, J. L., *Plastics Process Engineering*, Dekker (1979).
Walker, R. E., "Dragometer for Elastic Liquids," *ASME Symp. on Rheology*, 48 (1965).

Manuscript received May 24, 1982; revision received July 7, and accepted July 14, 1984.